Robust Opportunistic Optimal Energy Management of a Mixed Microgrid under Asymmetrical Uncertainties

Amal Nammouchi, Phil Aupke, Fabio D'andreagiovanni, Hakim Ghazzai, Andreas Theocharis, Andreas Kassler

Robust Opportunistic Optimal Energy Management of a Mixed Microgrid under Asymmetrical Uncertainties

Amal Nammouchi[a,*], Phil Aupke[a], Fabio D'Andreagiovanni[b,c], Hakim Ghazzai[d], Andreas Theocharis[e], Andreas Kassler[a]

[a] *Karlstad University, Computer Science Department, 65635 Karlstad, Sweden*
[b] *French National Centre for Scientific Research (CNRS), France*
[c] *Heudiasyc UMR 7253, Sorbonne Universités, Université, de Technologie de Compiègne, CNRS, CS 60319, 60203 Compiègne, France*
[d] *King Abdullah University of Science and Technology (KAUST), Thuwal, Saudi Arabia*
[e] *Karlstad University, Electrical Engineering Department, 65635 Karlstad, Sweden*

Abstract

Energy management within microgrids under the presence of large number of renewables such as photovoltaics is complicated due to uncertainties involved. Randomness in energy production and consumption make both the prediction and optimality of exchanges challenging. In this paper, we evaluate the impact of uncertainties on optimality of different robust energy exchange strategies. To address the problem, we present AIROBE, a data-driven system that uses machine-learning-based predictions of energy supply and demand as input to calculate robust energy exchange schedules using a multiband robust optimization approach to protect from deviations. AIROBE allows the decision maker to tradeoff robustness with stability of the system and energy costs. Our evaluation shows, how AIROBE can deal effectively with asymmetric deviations and how better prediction methods can reduce both the operational cost while at the same time may lead to increased operational stability of the system.

Keywords: Renewable Energy, Robust Optimization, Smart Grid, Machine Learning and AI

*Corresponding author
Email addresses: amal.nammouchi@kau.se (Amal Nammouchi), phil.aupke@kau.se (Phil Aupke), d.andreagiovanni@hds.utc.fr (Fabio D'Andreagiovanni), hakim.ghazzai@kaust.edu.sa (Hakim Ghazzai), andreas.theocharis@kau.se (Andreas Theocharis), andreas.kassler@kau.se (Andreas Kassler)

1. Introduction

The extensive use of fossil fuel-based energy, in order to meet the exponential energy-demand, has led to the depletion of these resources and an increase in greenhouse gas emissions. Towards neutral CO_2 societies and the achievement of the EU 2030 agenda, renewable energy sources (RES) and energy storage systems (ESS) are increasingly deployed to cover the electrification of the demand sector. Energy microgrids (MGs) of interconnected loads and distributed energy resources (DERs), e.g. RES, ESS, and electric vehicles, may connect to or disconnect from the upstream main grid aiming to secure the energy supply [1]. The dispersed nature of DERs leads prosumers to produce, store, consume, and exchange energy in a transactive operation that relieves the main grid and improves its stability and security to supply the demand [2, 3].

Microgrids (MGs) [4, 5] are small-scale power subsystems of the distribution grid that comprise generation capacities, storage devices, and controllable loads, operating as a single controllable system with self-supply and islanding capabilities [6]. In case of disturbances, the MGs can be isolated from the upstream network and sustain the supply of local loads through optimal management of the available resources, which are usually distributed. The optimization of the MG operations is extremely important in order to cost-efficiently manage its energy resources [7] and meet the demand. However, the power resulting from distributed renewable energy resources such as solar photovoltaic (PV) is stochastic and extremely reliant on the unpredictable and instantaneous fluctuation of the weather and the solar radiation [8]. The MGs optimization is also subject to the load uncertainty due the prosumer random behavior [9], the dynamic energy prices [10], and the physical constraints which impact the reliability and the the stability of the MG operation.

Several studies have suggested different mechanisms and solutions that increase the reliability and the performance of the MGs. For example, combining solar systems (or other RES) with energy storage systems (ESSs) such as batteries can significantly enhance the reliability of the MGs by storing the excess or covering the deficit [11, 12]. In such challenging environment, developing optimization algorithms that account for the system instability and cope with the different uncertainties is important [13, 14]. Similarly, intelligent production and load forecast schemes [15, 16] help improve the operational stability. Other methods to improve MGs operational efficiency are designing end-to-end MG architectures based on intelligent decision making [15] or deploying demand response based MGs [10, 17].

Optimal control is extensively used to determine the MGs operations. Contrary to deterministic optimization that assumes the different parameters are precisely known when optimizing the system, a robust modelling solution takes into account the above-mentioned uncertainties and constraints is needed in order to achieve an acceptable level of supply security and guarantee the MGs reliability [13]. In principle, stochastic programming (SO) and robust optimization (RO) can be used to deal with the MGs uncertainties. SO requires the knowledge of underlying probability distributions, which are often not known and must be estimated. However, wrong estimates lead to inaccurate solutions, and SO problems are typically computationally challenging and hard to solve. The alternative, RO, which addresses better the MG uncertainty settings, typically does not require information on the distribution of the uncertain parameters. Rather, knowledge on an uncertainty set is assumed. This includes all scenarios one wants to protect from, in a trade-off setting between the level of uncertainty and its effect on the objective function, the MGs cost in this case.

In order to address the issue of reliable and cost efficient scheduling, we propose in this paper AIROBE, which is a data-driven optimization model that protects against time-varying asymmetric deviations of predicted load and PV power generation. The goal from this work is to use machine-learning (ML)-based predictions as input to a less conservative robust optimization approach that accounts for both good and bad deviations instead of the absolute worst case, in opposition to the classical RO approaches. The specific contributions of this paper are as follows:

- We propose a tractable and comprehensive robust model to solve the optimal energy scheduling problem of a grid-connected mixed MG (residential and non residential users). The robust model accounts for the dynamicity of the energy prices and the uncertainties yielded from the PV generation and users' consumption profiles.
- We use variable uncertainty ranges for both the load and the PV generation that are computed with ML based forecast, for each time slot. The forecasting is based on pre-clustering method that clusters the data into sunny, rainy, overcast, and partial overcast days. The deviation ranges are strongly affected by this clustering, and impacts the energy scheduling and optimization.
- We propose a refined robust optimization approach for MGs scheduling under asymmetric load and PV generation uncertainties. In contrast to classical robustness model, the proposed robust model allows to take into account bad and good deviations over asymmetrical intervals, allowing

to obtain less conservative solution without sacrificing protection against uncertainty.
- The proposed solution is validated via simulations using real-world data set and evaluated using the price of robustness and the probability of the constraint violation in order to decide the trade-off between the cost and the energy balance violation. We demonstrate that our approach reduces the conservatism of the MG operation and decreases the MGs cost without impacting the constraint violation probability in comparison with the original budget-of-uncertainty model [18].

2. Motivation

To illustrate the uncertainties that may arise when using forecasts in the day-ahead optimization of energy exchanges in smart MGs, we trained different ML-based forecast models to predict PV production and energy consumption. Our models use clustering and consider the weather characteristics in order to increase model accuracy (more information in Section 4). Fig. 1 shows the different distributions of the forecast error (we use the Mean Absolute Percentage Error, MAPE) when predicting PV power generation (Fig. 1(a,c)) and energy consumption (Fig. 1(b,d)). The histogram is divided into over- (orange) and under-prediction (blue). Fig. 2 illustrates the variability of the deviation for the production and consumption prediction over time with a confidence interval of 80%. We summarize our main findings as follows:

- **Different weather conditions result in different error characteristics:** the deviations of observed values from predicted ones in terms of under- and over predictions behave differently for each of the weather conditions (see Fig. 1). For example, when observing the prediction error for PV production and consumption for the partly overcast days, we notice a trend for larger negative deviation of the observed values from the predicted values leading to higher under prediction. However, for sunny days, there is a trend toward over prediction of both energy supply and demand.
- **Asymmetrical deviation:** the deviation, i.e., the difference between predicted value and observed value of the PV production and the prosumer consumption is asymmetrical, i.e, the lower and the upper bounds of the deviations are not equal as shown in Fig. 1.
- **Uncertainty varies over different prediction horizons:** Fig. 2) plots deviations of predicted values from observed values for both PV production and energy consumption of a single prosumer over a whole

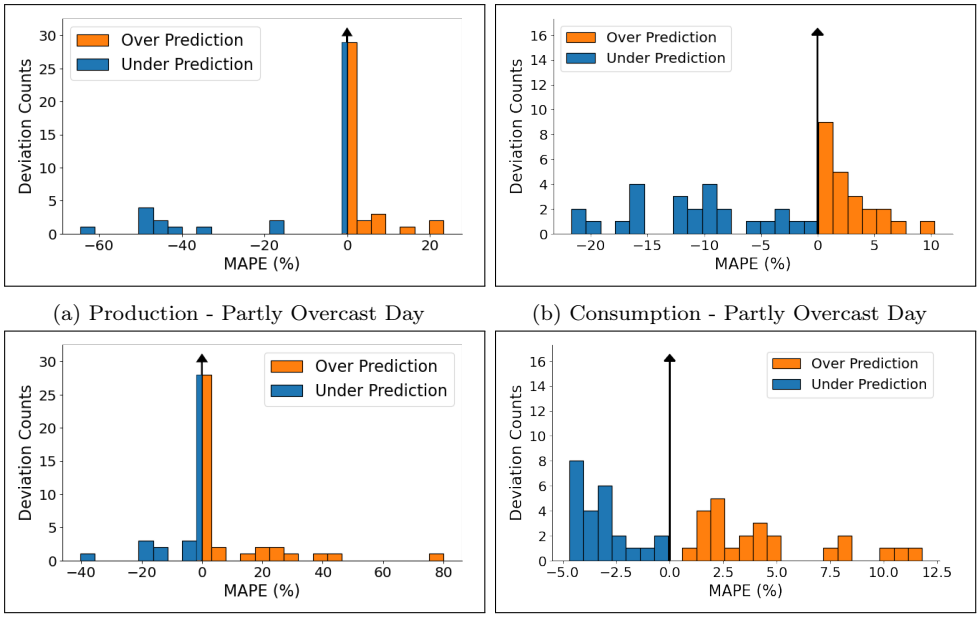

(a) Production - Partly Overcast Day

(b) Consumption - Partly Overcast Day

(c) Production - Sunny Day

(d) Consumption - Sunny Day

Figure 1: Distribution of over- and under prediction in terms of MAPE for one prosumer PV power generation and energy consumption during 24 hours

day. As can be seen, the deviation range and asymmetry varies over different timeslots.

Based on these observations, we conclude that the MGs operation may be severely impacted by asymmetric time-varying deviations caused by the uncertainties involved when predicting both the PV power generation and the prosumers consumption. Given these uncertainties, the MGs scheduling problem can be categorized as an optimization problem with resource uncertainty, where the predicted consumption and production have uncertain upper and lower bounds for each time slot. Due to these deviations, the worst-case scenario happens when the realized PV power generation is lower than expected, or alternatively, when the consumption is higher than predicted. These deviations can be described as bad deviations for our system.

In fact, if the MGs scheduling is planned solely based on predicted values, even small prediction errors and uncertainties associated with the demand and the available power can make the planned power dispatch infeasible, potentially lead to high operational costs (e.g., due to unplanned high demand or low supply), and may lead to security and reliability issues in the power system when using the predicted values for the MGs operation in real-time.

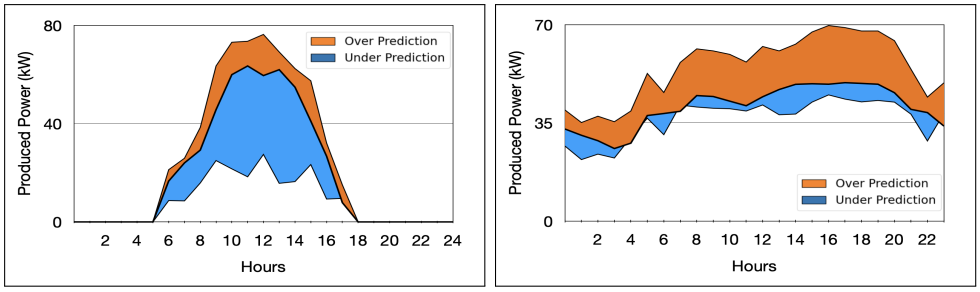

(a) Asymmetrical Deviation - PV Power Production

(b) Asymmetrical Deviation - Energy Consumption

Figure 2: Deviations for one prosumer PV power generation (a) and energy consumption (b) during 24 hours

Alternatively, as shown in Fig. 1, the true available PV power may be much higher than the predicted value (i.e., power underprediction case) and the consumption can be lower than expected (i.e., overprediction case). These deviations can be described as good deviations. In this case, using a worst-case scenario based scheduling using predicted values means that the total available power may never be entirely utilized by the MGs and that the planned decisions are overly conservative and may also entail high costs.

Furthermore, Fig. 2 illustrates, that the deviation of a day-ahead prediction is variable over time and is not constant or symmetrical. Hence, our proposed approach must be able to optimize the MGs energy scheduling under time-varying and asymmetric deviations. As a consequence, we need to formulate our model so that it protects against the bad deviations and removes the unnecessary protection by taking advantage of the good deviations in an opportunistic less conservative manner.

3. Modelling the MG Energy Exchange Optimization Problem

We consider an MG made up of a cluster of prosumers and consumers that are geographically close. Each prosumer is equipped with a battery, a PV cell, and is associated with a power load. Each consumer is associated with a power load. It is not equipped with a PV cell but may possess a battery (e.g., for electric vehicles or load coverage). The prosumers and consumers can exchange power (import/export, i.e., buy/sell) among each other, and the MG can exchange power with the main grid to cover its demand or to sell its surplus. The prices of power imports and exports are dynamic (i.e., they may vary over the time periods constituting the planning horizon that we consider).

Given a time horizon decomposed into a set of time periods T and given

an MG including a set C of users (prosumers or consumers), the optimal MG exchange problem that we consider is that of choosing the charge/discharge actions of each user and import/export actions of the MG in each time period, satisfying the total MG load constraint while taking into account the PV generation and the state-of-the-energy constraints, with the aim of miminimizing the total cost of the MG over the horizon. In this work, we assume that battery degradation and leakage effects are negligible.

3.1. Deterministic Optimization Model

We start by defining the deterministic model, which does not take into account the uncertainty of users' loads and PV generation. The model involves the following decision variables:

- binary variables $y_t^{im} \in \{0,1\}$, $\forall t \in T$, which are equal to 1 if power is imported by the MG in period t and 0 otherwise;
- binary variables $y_t^{ex} \in \{0,1\}$, $\forall t \in T$, which are equal to 1 if power is exported by the MG in period t and 0 otherwise;
- continuous variables $p_t^{imp} \geq 0$, $\forall t \in T$ that represent the amount of power imported in each period t;
- continuous variables $p_t^{exp} \geq 0$, $\forall t \in T$ that represent the amount of power exported in each period t;
- binary variables $x_{j,t}^{ch} \in \{0,1\}$, $\forall j \in J, t \in T$, which are equal to 1 if the battery of user j is charged in period t and 0 otherwise;
- binary variables $x_{j,t}^{dis} \in \{0,1\}$, $\forall j \in J, t \in T$, which are equal to 1 if the battery of user j is discharged in period t and 0 otherwise;
- continuous variables $b_{j,t}^{ch} \geq 0$, $\forall t \in T$ that represent the amount of charge of user j's battery in period t;
- continuous variables $SoE_{j,t} \geq 0$, $\forall t \in T$ that represent the state of energy of user j's battery in period t.

These decision variables are employed in a number of constraints. First, we must express the link between the charge (discharge) binary and continuous variables, imposing that the continuous charge (discharge) variables of a user $j \in C$ in period $t \in T$ cannot exceed an upper bound k_j^{ch} (k_j^{dis}) when a charge (discharge) occurs in a period:

$$b_{j,t}^{ch} \leq k_j^{ch} \cdot x_{j,t}^{ch} \qquad \forall j \in C, t \in T\,, \tag{1}$$

$$b_{j,t}^{dis} \leq k_j^{dis} \cdot x_{j,t}^{dis} \qquad \forall j \in C, t \in T\,. \tag{2}$$

Furthermore, we must express that a user j can either charge or discharge its battery in each period t, i.e.:

$$x_{j,t}^{ch} + x_{j,t}^{dis} \leq 1 \qquad \forall j \in C, t \in T \; . \tag{3}$$

Similarly, we must express the variable upper bound Imp_t (Exp_t) on the power that may be imported (exported) in each time period $t \in T$ and the condition of either importing or exporting in each period, i.e.:

$$p_t^{im} \leq \mathrm{Imp}_t \cdot y_t^{imp} \qquad \forall t \in T \; , \tag{4}$$

$$y_t^{im} \leq Exp_t \cdot y_t^{exp} \qquad \forall t \in T \; , \tag{5}$$

$$y_t^{im} + y_t^{ex} \leq 1 \qquad \forall t \in T \; . \tag{6}$$

We also include constraints on the State of Energy (SoE), linking the value of SoE variables to the energy variation occurring between consecutive time periods (here Δt is the duration of a time period) and imposing bounds SoE_j^{min}, SoE_j^{max} on the minimum and maximum values that an SoE variable may assume:

$$SoE_{j,t} = SoE_{j,t-1} + (b_{j,t-1}^{ch} - b_{j,t-1}^{dis}) \cdot \Delta t \qquad \forall j \in C, t \in T \; , \tag{7}$$

$$SoE_j^{min} \leq SoE_{j,t} \leq SoE_j^{max} \qquad \forall j \in C, t \in T \; . \tag{8}$$

Eventually, we define the load constraints imposing that, for each period $t \in T$, the sum of the power $p_{j,t}^{PV}$ produced through PV by each user $j \in J$ plus the sum of the charge/discharge variation of batteries of all users and the import/export variation with the main grid must be greater or equal than the sum of the load $p_{j,t}^{PC}$ of the users, i.e.:

$$\sum_{j \in C} \left[p_{j,t}^{PV} + \left(b_{j,t}^{dis} - b_{j,t}^{ch} \right) \right] + \left(p_t^{imp} - p_t^{exp} \right) \geq \sum_{j \in C} p_{j,t}^{PC} \qquad \forall t \in T \; . \tag{9}$$

The objective is to minimize the total cost of power import/export over the entire time horizon, obtained by summing the difference between the cost of importing (with price π_t^{im}) and the revenue of exporting (with price π_t^{ex}):

$$\min \; \sum_{t \in T} (\pi_t^{im} \cdot p_t^{im} - \pi_t^{ex} \cdot p_t^{ex}) \; . \tag{10}$$

3.2. Robust Optimization Model

The previous model is deterministic and neglects the fact that both the load coefficients $p_{j,t}^{PC}$ and PV power generation coefficients $p_{j,t}^{PV}$ of constraints (9)

are subject to uncertainty and their exact value is not known in advance. In order to tackle such data uncertainty, which may lead to infeasibility and severe suboptimality of solutions when neglected and not properly taken into account in the model (see [19] for an exhaustive discussion), we propose to adopt a Robust Optimization (RO) approach. RO is a methodology that takes into account data uncertainty under the form of hard constraints that are added to the model for considering only *robust solutions*, namely solutions whose feasibility is preserved even when data deviations specified by an uncertainty set occur.

We start by considering a classical RO model, so called Γ-Robustness [18] for then proposing an improved RO model that allows to more accurately represent data deviations. In a more formal way, in an RO approach: 1) the *actual value* of an uncertain coefficient is supposed to equal the summation of a reference value *nominal value* set by the decision maker and an unknown deviation; 2) an *uncertainty set* is defined for specifying all possible deviations for which protection is required; 3) it is defined a *robust counterpart*, namely a modified version of the original deterministic optimization problem that includes only robust solutions. Granting robustness comes at the so-called *price of robustness*, which is a degradation in the optimal value caused by excluding non-robust solutions from the feasible set. In general, increasing robustness and thus adding protection against uncertainty leads to a higher price of robustness.

In the optimization model presented in Subsection 3.1, the uncertainty affects the load constraints (9): following the Γ-Robustness approach, we assume that the actual value of each uncertain load coefficient $p_{j,t}^{PC}$ and of each PV power generation coefficient $p_{j,t}^{PV}$ falls in the symmetric intervals:

$$\begin{aligned} p_{j,t}^{PV} &\in [\bar{p}_{j,t}^{PV} - \delta_{j,t}^{PV}, \bar{p}_{j,t}^{PV} + \delta_{j,t}^{PV}] \\ p_{j,t}^{PC} &\in [\bar{p}_{j,t}^{PC} - \delta_{j,t}^{PC}, \bar{p}_{j,t}^{PC} + \delta_{j,t}^{PC}] \end{aligned} \tag{11}$$

where $\bar{p}_{j,t}^{PV}$, $\bar{p}_{j,t}^{PC}$ are the nominal values and $\delta_{j,t}^{PV}, \delta_{j,t}^{PC}$ the corresponding maximum deviation. Furthermore, the approach provides for introducing parameters $\Gamma_t^{PV} \in \{0, |J|\}$, $\Gamma_t^{PC} \in \{0, |J|\}$ denoting the number of load and PV generation coefficient deviations for which protection is requested in each period $t \in T$. These parameters represent a budget of uncertainty and allow to control the level of protection against uncertainty and the corresponding price of robustness: when $\Gamma_t = 0$ no protection is imposed and the price of robustness is null; by increasing the value of Γ_t, the protection and the price of robustness increase, until reaching full protection for $\Gamma_t = |J|$, which also entails the highest price of robustness.

Using the theoretical results of Γ-Robustness presented in [18], we can write the following robust counterpart of the constraints (9):

$$\sum_{j\in C}\left[\bar{p}_{j,t}^{PV}+\left(b_{j,t}^{dis}-b_{j,t}^{ch}\right)\right]-\left(\Gamma_t^{PV}\cdot v_t^{PV}+\sum_{j\in C}w_{j,t}^{PV}\right)+\left(p_t^{imp}-p_t^{exp}\right)$$
$$\geq\sum_{j\in C}\bar{p}_{j,t}^{PC}+\left(\Gamma_t^{PC}\cdot v_t^{PC}+\sum_{j\in C}w_{j,t}^{PC}\right)\qquad\forall t\in T\ , \quad (12)$$

$$v_t^{PV}+w_{j,t}^{PV}\geq\delta_{j,t}^{PV}\qquad\forall j\in C,t\in T\ , \quad (13)$$
$$v_t^{PC}+w_{j,t}^{PC}\geq\delta_{j,t}^{PC}\qquad\forall j\in C,t\in T\ , \quad (14)$$
$$v_t^{PV},\ v_t^{PC}\geq 0\qquad\forall t\in T\ , \quad (15)$$
$$w_{j,t}^{PV},w_{j,t}^{PC}\geq 0\qquad\forall j\in C,t\in T\ . \quad (16)$$

which is made up of: i) the robust constraint (12), which is a modified version of (9) that refers to the nominal coefficient values $\bar{p}_{j,t}^{PV}$, $\bar{p}_{j,t}^{PC}$ and includes additional terms modelling the deviations of coefficients and the Γ parameters controlling robustness; ii) auxiliary constraints (13), (14) and auxiliary variables (15), (16) introduced by the procedure of [18] exploiting duality theory of Linear Programming.

3.3. A refined robust model considering asymmetrical and "good" deviations

While Γ-Robustness constitutes the most successful method for Robust Optimization and still represents a major reference that is widely used in a vast number of real-world uncertain optimization problems (see e.g, [19]), it offers opportunities for improvements. Here, we attempt at obtaining a more refined representation of uncertainty, reducing the price of robustness without sacrificing protection, by considering an asymmetrical range of deviation of the coefficients and taking into account "good" deviations in the value of coefficients. By "good" deviations, we intend favourable deviations in the value of coefficients, like an increase in the PV power production $p_{j,t}^{PV}$ or a reduction in the load $p_{j,t}^{PC}$, which strengthen feasibility instead of leading towards infeasibility: these deviations are indeed likely in reality, but are completely neglected by Γ-Robustness, which considers only worst-case "bad" deviations leading towards infeasibility.

As first step, we define the following modified deviation ranges:

$$p_{j,t}^{PV}\in[\bar{p}_{j,t}^{PV}-\delta_{j,t}^{PV-},\bar{p}_{j,t}^{PV}+\delta_{j,t}^{PV+}]$$
$$p_{j,t}^{PC}\in[\bar{p}_{j,t}^{PC}-\delta_{j,t}^{PC-},\bar{p}_{j,t}^{PC}+\delta_{j,t}^{PC+}] \quad (17)$$

in which the range is asymmetrical and the value of the largest negative deviations $\delta_{j,t}^{PV-}, \delta_{j,t}^{PC-}$ and positive deviations $\delta_{j,t}^{PV+}$ $\delta_{j,t}^{PC+}$ do not have to coincide, as common in real-world optimization under uncertainty [20].

The classical Γ-robust model is able to take into account only the "bad" deviations $\delta_{j,t}^{PV-}$ (decrease in the PV generation) and $\delta_{j,t}^{PC+}$ (increase in the load) and leads towards the infeasibility of the load constraint (9). If we want to take into account the "good" deviations $\delta_{j,t}^{PV+}$ (increase in the PV production) and $\delta_{j,t}^{PC-}$ (decrease in the load), it is necessary to extend the Γ-robust model, in particular introducing an additional parameter Θ_t specifying the minimum number of deviations that must be "good" and suitable associated constraints.

When considering the "good" deviations together with the "bad" deviations, we can prove the following results:

Proposition 1. *For each time period $t \in T$, the robust counterpart of constraint (9) when protection for Γ_t^{PV} "bad" deviations and Θ_t^{PV} "good" deviations of PV generation coefficients and Γ_t^{PC} "bad" deviations and Θ_t^{PC} "good" deviations of load coefficients are allowed in period t writes as:*

$$\sum_{j\in C}\left[\bar{p}_{j,t}^{PV}+\left(b_{j,t}^{dis}-b_{j,t}^{ch}\right)\right]-\left(\Gamma_t^{PV}\cdot v_t^{PV-}-\Theta_t^{PV}\cdot v_t^{PV+}+\sum_{j\in C}w_{j,t}^{PV}\right)$$
$$+\left(p_t^{imp}-p_t^{exp}\right)\geq\sum_{j\in C}\bar{p}_{j,t}^{PC}+\left(\Gamma_t^{PC}\cdot v_t^{PC+}-\Theta_t^{PC}\cdot v_t^{PC-}+\sum_{j\in C}w_{j,t}^{PC}\right) \quad (18)$$

$$v_t^{PV-}+w_{j,t}^{PV}\geq\delta_{j,t}^{PV-} \qquad \forall j\in C \quad (19)$$
$$-v_t^{PV+}+w_{j,t}^{PV}\geq-\delta_{j,t}^{PV+} \qquad \forall j\in C \quad (20)$$
$$v_t^{PC+}+w_{j,t}^{PC}\geq\delta_{j,t}^{PC+} \qquad \forall j\in C \quad (21)$$
$$-v_t^{PC-}+w_{j,t}^{PC}\geq-\delta_{j,t}^{PC-} \qquad \forall j\in C \quad (22)$$
$$v_t^{PV+},\ v_t^{PV-}\geq 0 \quad (23)$$
$$w_{j,t}^{PV}\geq 0 \qquad \forall j\in C \quad (24)$$
$$v_t^{PC+},\ v_t^{PC-}\geq 0 \quad (25)$$
$$w_{j,t}^{PC}\geq 0 \qquad \forall j\in C \quad (26)$$

Proof. For the proof, we refer the reader to Appendix A. □

4. Prediction of PV Energy Supply and Demand

AIROBE requires as input the prediction of PV Energy Supply and Demand as well as its deviation ranges for each forecast interval. We use data-driven approaches for obtaining model input as described below.

Data pre-processing. AIROBE integrates data cleaning techniques to improve data quality for making predictions of high quality. To detect outliers and missing data we are using interquartile range (IQR) method. Data points, which are not within a percentile of the mean are detected as outliers and replaced by the average of previous/future values. For the solar PV production, we also remove the night times, since they are not relevant for the prediction of solar energy production [21].

Weather type clustering. Previous work in this field has shown, that four clusters for the weather types (sunny, partly overcast, overcast and rainy) perform the best [22]. We cluster the data using the weather features available in the dataset (solar irradiation, temperature and humidity for the whole year) using K-means clustering in combination with dynamic time warping (DTW) to create the clusters. DTW has shown superior performance when applied to time-series datasets, because it is able to detect similar patterns even if they do not occur in the same time period [23].

Forecasting Models. We enrich the clustered datasets with the historical information about the PV power production and energy consumption of the prosumer in the system. For each of the four clusters we then generate an individual machine learning forecast model. As a predictor we use LightGBM, which is a gradient boosting decision tree (GBDT) algorithm [24]. LightGBM is constructed differently than conventional GBDT algorithms, as it grows leaf-wise to find a leaf with the largest split gain instead of iterating over all previous leaves. To additionally speed up the training of the model it uses advanced networking communication called parallel voting decision tree algorithm, which enables parallel computation during the training process [25, 26]. Since the LightGBM regressor only supports single-step forecasting, we additionally wrapped an auto-regressive direct multi-step forecaster [27], which generates the multi-step forecast in a sliding window manner. This means, that the model predicts the next time slot and uses that prediction as an additional input for the next step in an iterative manner.

Prediction Interval. Since the prediction of time-series data is probabilistic, it is necessary to determine the possible deviation of the forecast. AIROBE needs for each prediction interval the range of the deviation as input in order to optimize the exchange of energy in the system for the next period. We

use quantile regression (QR) to elaborate the prediction deviation [28]. QR can be described as follows: $Q_y\left(q \mid X_t\right) = X_t\beta_q$. $Q_y(q|*)$ is the conditional q^{t} quantile of the production or consumption distribution (y_t). X_t are the regressors for each quantile, while β_q represents the vector of parameters for the quantile q. Each of the two predictors for the quantiles use the pinball loss function or quantile score (QS), present in (27).

$$\varphi\left(y_t, \widehat{y}_{t,q}, q\right) = \begin{cases} \left(1 - \frac{q}{100}\right)\left(\widehat{y}_{t,q} - y_t\right) & y_t < \widehat{y}_{t,q} \\ \frac{q}{100}\left(y_t - \widehat{y}_{t,q}\right) & y_t \geq \widehat{y}_{t,q} \end{cases} \tag{27}$$

$\widehat{y}_{t,q}$ is the q^{t} quantile of the predicted load and consumption and y_t is the target value for each prediction. The QS is the mean of the pinball losses across all target quantiles [29].

Error Metric. We used the Mean Absolute Percentage Error (MAPE) to evaluate the prediction quality of the machine learning models:

$$MAPE = \frac{1}{n}\sum_{t=1}^{n}\left|\frac{A_t - F_t}{A_t}\right| * 100 \tag{28}$$

where A_t represents the vector of the actual values, F_t the forecasted ones and n is the number of predictions.

5. Evaluation

In this section we answer the following questions:

1. *Prediction Interval*: How accurate are our clustering-based ML-models in predicting the PV power generation, the energy consumption and what is the resulting deviation over time for different clusters?
2. *Robustness*: How do different parameters of AIROBE impact the robustness of the solution, the cost and the state of energy?
3. Price of Robustness: How can AIROBE reduce the Price of Robustness (PoR) and what is the impact of the opportunistic model on constraint violation probability?

5.1. Baselines

We use the following baselines for analysis and comparison with the proposed AIROBE model: we use the partial knowledge based model as

described in the subsection.3.2 as baseline which considers uncertainty in both the load and the PV production sides. We call this conventional robust approach which considers the absolute worst-case of PV production and prosumer consumption under a budget of uncertainty.

5.2. Experimental Setup

5.2.1. Data set

In this study, we validate the effectiveness of the forecasting and scheduling models on the city learn framework data set[1]. The data set contains $n = 9$ residential and non-residential users subscribing in the EMS. The load represents the heating and the appliances demand. The data set contains the hourly consumption and PV power generation for the different users and the weather information during one year.

5.2.2. PV power generation and energy consumption prediction

The sub-datasets for the four different clusters were divided into a training (75%) and testing (25%) dataset. A LightGBM model was trained for the energy consumption and PV power production of each prosumer and weather cluster, individually. The predictor takes 48 hours as input to forecast the next 24 hours. Additionally, we used grid-search to select the best hyperparameters for each model. To estimate the deviations of the prediction we used the QR and QS as described in section 4 using 0.90 for the upper boundary and 0.10 for the lower one to build a 80% confidence interval.

5.2.3. Optimization

In our case study, we schedule day-ahead energy exchange where each time slot is equal to 1 hour; with time horizon of $N = 24$ hours i.e, the decision is made by solving the optimization problem for the next $N = 24h$ with a time window from 0:00 to 23:59. Hourly import and export prices were obtained from Nord Pool market data[2]. We use the ML predictions for the PV production, the consumption and their deviations as the input to our optimization models, i.e, the reference values. The model is implemented in python and solved by Gurobi.

5.3. Prediction Quality

Table 1 shows the prediction quality of the produced PV energy for prosumer nine. The table shows the average deviation for the under and

[1] https://github.com/intelligent-environments-lab/CityLearn
[2] https://www.nordpoolgroup.com

Table 1: Production summary for prosumer nine

Cluster	Average Deviation		Overall Maximum Deviation	Overall Minimum Deviation	MAPE
	Over Prediction	Under Prediction			
Rainy	12.97%	21.97%	23.35%	1.15%	5.63%
Partly Overcast	15.87%	11.46%	40.31%	1.24%	3.22%
Sunny	30.21%	4.16%	40.42%	1.32%	2.06%
Overcast	54.74%	0.17%	83.09%	0.53%	5.69%

Table 2: Consumption summary for prosumer nine

Cluster	Average Deviation		Overall Maximum Deviation	Overall Minimum Deviation	MAPE
	Over Prediction	Under Prediction			
Rainy	18.72%	16.67%	39.28%	4.03%	6.60%
Partly Overcast	17.54%	26.68%	21.28%	4.19%	8.56%
Sunny	9.48%	3.93%	29.91%	1.61%	4.32%
Overcast	30.05%	18.79%	46.55%	3.15%	5.83%

over prediction, overall maximum and minimum deviation in percentage and MAPE over the period of 90 days for the weather type clusters. It is visible that the clusters behave differently. For example, the sunny cluster has a stronger deviation towards the over prediction with an average deviation of 30.21% while the average under prediction is 4.16%. This behaviour of good deviations is also visible in the overcast weather cluster. The other weather clusters average deviation for the under and over prediction express a mostly even magnitude towards either bound. In terms of the prediction quality, the sunny cluster has the lowest MAPE of 2.06%. The overcast cluster presents the highest overall maximum deviation of 54.74%. The high maximum deviation occurs when there is a sudden change in the power production. This means, that the day is for example clustered as an overcast day, but the production of the PV panel is higher than predicted due to sudden weather changes (see Fig. 4 and Fig. 3).

Table 2 summarizes the prediction quality for the energy consumption. In contrast to the prediction of the PV generation, the MAPE is higher in every weather cluster. However, this is not visible in terms of deviations. The sunny cluster for example, still shows a stronger magnitude in deviation towards the over prediction with 9.48% but it is lower than the 30.21% in table 1 for the production.

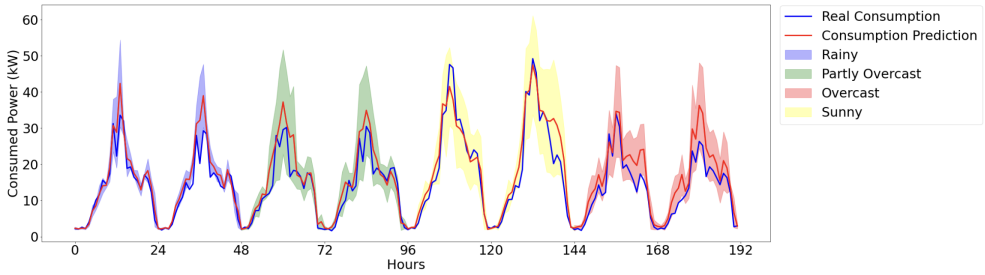

Figure 3: Consumption prediction and deviation of prosumer nine for each weather cluster.

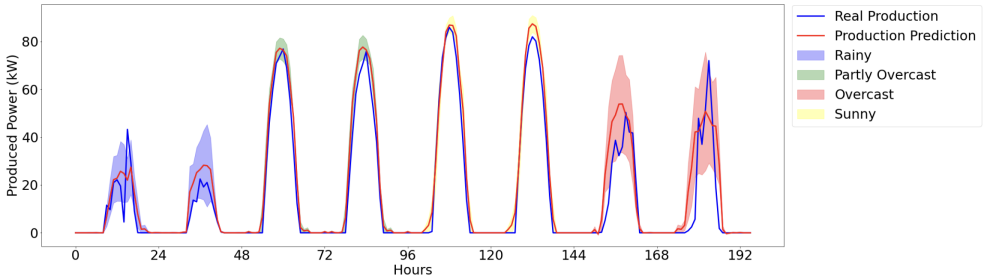

Figure 4: Production prediction and deviation of prosumer nine for each weather cluster.

5.4. Robustness

In order to study the impact of the proposed model AIROBE on the objective value, i.e, the MG operational cost, we evaluate the cost under the different types of budget of uncertainty namely: Γ_t^{PV}, Θ_t^{PV}, Γ_t^{PC}, Θ_t^{PC}. We plot the MG aggregated cost in Fig.5. First, we optimize using the baseline worst-case model under the PV production and consumption uncertainties described in 3.2 and we plot the results in Fig.5.(c). We observe that the cost value increases with the increase of the uncertainty budgets Γ_t^{PV} and Γ_t^{PC}. The values $(\Gamma_t^{PV}, \Gamma_t^{PC}) = (0, 0)$ corresponds to the deterministic baseline described in 3.1 where we don't have any protection. In this deterministic case, we have the lowest cost 2399.89€/kWh, however, the future deviations will cause the MG to import on the spot in order to cover the demand which will cause an instability of the MG and yields higher expected cost in the future. The values $(\Gamma_t^{PV}, \Gamma_t^{PC}) = (9, 9)$ correspond to the most-conservative case where we protect from all possible deviation to their lower bounds which yields the highest possible cost 5007.48€/kWh. The high cost is explained by the fact that when we protect from the worst case scenario, we expect to produce less, alternatively consume more, which leads the users to import more power and charge their batteries to cover the future demand.
In Fig.5.(a),(b). we optimise using the proposed model AIROBE described

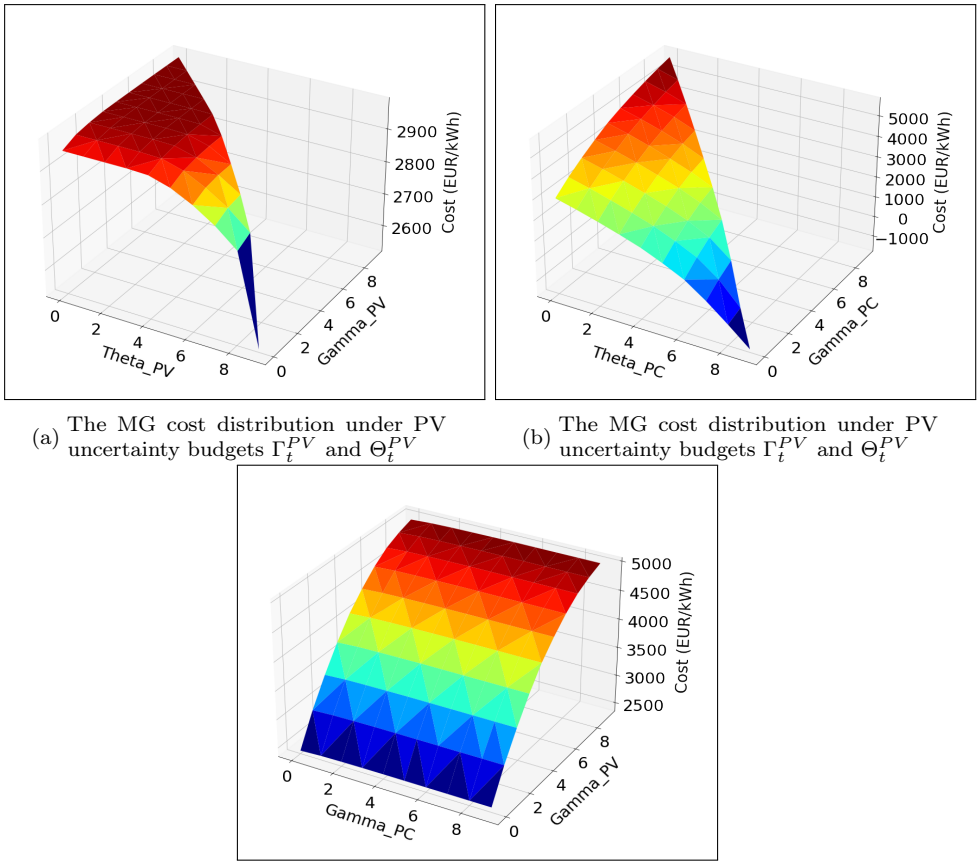

(a) The MG cost distribution under PV uncertainty budgets Γ_t^{PV} and Θ_t^{PV}

(b) The MG cost distribution under PV uncertainty budgets Γ_t^{PV} and Θ_t^{PV}

(c) The MG cost distribution under PV uncertainty budgets Γ_t^{PV} and Γ_t^{PC}

Figure 5: The MG cost distribution under different types of uncertainty.

in 3.3. In Fig.5.(a). we study the impact of the budgets related to the PV generation uncertainty. We observe that the cost has the highest values when $\Theta_t^{PV} = 0$ which represents the same values as in Fig.5.(c). for $\Gamma_t^{PC} = 0$ and corresponds to the baseline value where we don't consider the favourable deviations. In Fig.5.(a)., the cost increases as we increase the budget Γ_t^{PV} for a fixed Θ_t^{PV}. We notice that the cost value decreases as we increase the budget Θ_t^{PV} and hits the minimum value 2527.71€/kWh for $(\Theta_t^{PV}, \Gamma_t^{PV}) = (9, 0)$. In fact, by introducing the budget Θ_t^{PV} which reflects the favourable deviations, the users tend to be more opportunistic and import less compared to the worst-case scenario where they import more than their demand and charge their batteries in order to protect from future worst deviations. However, in

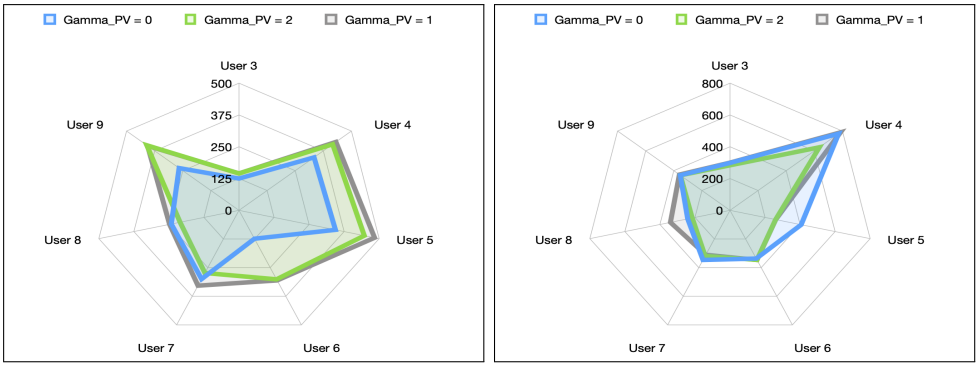

(a) Overall State of Energy of seven users for $\Gamma_t^{PV} = 0, 1, 2$ and $\Theta_t^{PV} = 0$

(b) Overall State of Energy of seven users for $\Gamma_t^{PV} = 0, 1, 2$ and $\Theta_t^{PV} = 2$

Figure 6: The impact of the different budgets of uncertainty on the overall State of Energy (kWh) of the prosumers batteries.

a sunny day for example, the PV generated power is likely to deviate to its upper bound as shown in 2. Taking those scenarios into account, makes the scheduling less conservative and reduces the extensive import from the main grid that appears in the worst-case scenario based scheduling.
Similarly, in Fig.5.(b). we plot the aggregated MG cost under the impact of the budgets related to the users consumption uncertainty. The negative values of the cost corresponds to a profit where the MG is expected to make a profit. This scenario might appear when the MG has power generation excess in comparison to the consumption, and the model takes into account these favorable good deviations while (The users produce more than expected or consume less than expected). We observe that the two budgets of uncertainty have similar affect on the cost as in Fig.5.(a) where the cost decreases as we increase the budget Θ_t^{PC}. This is explained by the fact that the users consumption might deviate to its lower bound, i.e, the user consume less energy than the predicted value and taking that into account encourages them to import less or charge their batteries less. We can conclude that integrating the favourable deviations into the scheduling, yields lower cost which implies lower power import from the main grid in general.

Fig.6. presents the aggregated state of the energy (SoE) of seven users, and its variation under different budgets of uncertainty. In Fig.6.(a). we fix $\Theta_t^{PV} = 0$ and optimize for three different budgets of uncertainty related to the PV power generation Γ_t^{PV}. We pick one sunny day in order to showcase the effectiveness of the budget of uncertainty related to the favourable deviations. We observe that the users batteries tend to have a higher SoE when we

increase the value of Γ_t^{PV} in Fig.6.(a). In fact, in order to protect from the worst-case scenario, i.e, the bad deviations, the users tend to charge their batteries to replace the expected deficit. In Fig.6.(b). we want to assess the impact of the favourable deviations on the battery behavior. We fix $\Theta_t^{PV} = 2$, i.e, the model will take into account that two uncertain parameters will deviate to their upper bound. We observe that the SoE has increased in general. This is due to the fact that higher expected generated PV power were taken into account in the optimization scheduling and the users charge their batteries with that excess or provide it to the MG utilization which means other users with deficit will tend to charge their batteries as well.

5.5. Price of Robustness

To show the impact of data uncertainty on the objective value, i.e, the MG operational cost, and to demonstrate the effectiveness of the proposed approach against it, we simulate 10000 scenarios of random yields for users production and then we compare the robust solutions generated by varying the level of the uncertainty budgets Γ_t^{PV} and Θ_t^{PV}. For simplification and without loss of generality, we fix Γ^{PC} and Θ_t^{PC} to zero. We evaluate the constraint violation probability and the Price of Robustness. We define the PoR rate as the relative difference between the costs realized by the robust solution and the nominal solution where we don't protect against the uncertainty. The PoR is used to quantify the extra MG cost required to cover for the robust solution. We calculate the PoR as follow:

$$PoR = 100\frac{Cost_{\Gamma=0} - Cost_{\Gamma>0}}{Cost_{\Gamma} = 0} \tag{29}$$

Fig. 7.(a). shows the PoR rate variation as we increase the worst-case scenario budget of uncertainty Γ_t^{PV} for different fixed values of Θ_t^{PV}. The case where $\Theta_t^{PV} = 0$, which corresponds to the baseline model (approach 3), yields the highest value of PoR, alternatively the highest cost. The value of PoR increases as we increase the budget Γ_t^{PV} since we are protecting more against the worst-case scenario, where the higher Γ_t^{PV} the more uncertain variables deviate to their lower bound corresponding to less PV power production. In Fig. 7.(a). we compute the PoR for different values of Θ_t^{PV} which indicates that some uncertain variables will deviate to their upper bound, i.e, the PVs will generate more power then expected, which mostly corresponds to sunny days. The PoR is reduced as we introduce the good deviations in our scheduling. The objective value is reduced by 0.82% atmost for $\Theta_t^{PV} = 4$ compared to 1.92% PoR for the classical worst-case model, i.e, $\Theta_t^{PV} = 0$.

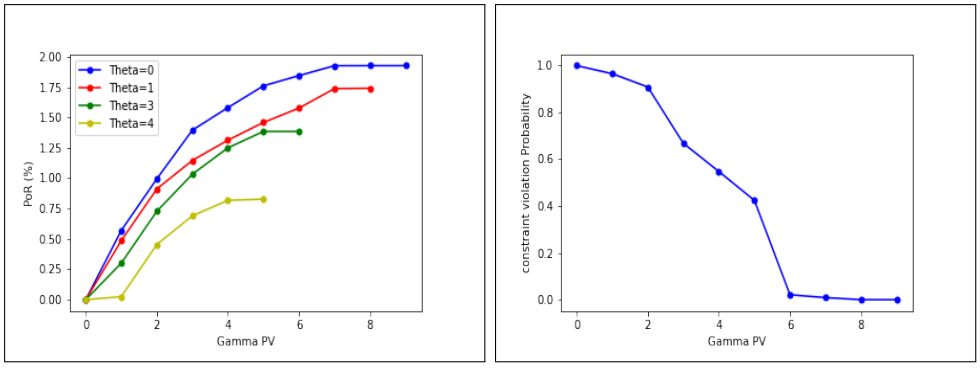

(a) Price of Robustness rate for different values of good deviation budgets Θ_t^{PV}

(b) Probability of Constraint Violation for different values of Θ_t^{PV}

Figure 7: Evaluation of the AIROBE robustness performance in terms of the good and bad deviations

Fig. 7.(b). illustrates the probability of constraint violation for different levels of protection Γ_t^{PV}. The probability of constraint violation decreases when we increase the level of protection until it reaches the value 0. This is explained by the fact that the more we protect against the uncertainty, the more probable it is that we achieve energy balance and meet our demand. We note that we compute the probability of constraint violation for the different values of Θ_t^{PV}, which remains unchangeable. We conclude that the proposed model reduces the PoR and exhibit lower MG costs while conserving the same level of protection.

6. Limitations and Next Steps

AIROBE took an initial step in formulating a robust MGs energy scheduling model, that accounts for time-varying prediction uncertainties. Compared to classical Γ-robustness models, we consider asymmetric uncertainty ranges under bad and good deviations, which allows us to calculate more opportunistic solutions. In this section, we describe limitations of the current model and possible future directions.

AIROBE assumes that the battery capacity is constant and neglects the degradation of the battery life over time because we evaluate our scheduling over a short period of time. In real life, the battery is impacted by the charging and discharging cycles and degrades over time which can impact both the cost and the solver decisions. Adding such battery constraints, a battery-related cost to the objective function and evaluating over a long period of time is a possible next step in this work. While our current model assumes that the different uncertain parameters are independent, the PV power generation

and less so the load profiles maybe subject to geographical and temporal correlation. AIROBE can be extended to consider the correlation of the uncertain parameters and study its impact on the robustness and the budget of uncertainty, in a multi-microgrids settings. Finally, an area of further research is to extend AIROBE for other DERs such as wind power and consider the curtailment cost.

7. Related Work

There are several related works in the area of optimization of MG operations [30, 31], under different modes; centralized [32] and decentralized [33], using different modelling approaches for MG operations and management systems. These approaches can be categorized into two types: model-driven and data-driven based modelling solutions.

For the model-driven approaches, [34, 35] developed a mixed integer linear programming solution (MILP), while the authors in [36, 37] proposed a mixed integer non linear programming (MINLP) solution for operational planning and optimal sizing of MGs. [38] used dynamic programming for optimal energy management of a standalone MG. Metaheuristics and heuristics such as memory-based Genetic Algorithms [39] and Tabu Search [40] have been proposed to solve the power dispatch problem for MGs which provides faster yet sub-optimal solution. In contrast to our work, those approaches assume perfect knowledge about the future without protecting against uncertainties, which may not be available in practice.

Examples of data-driven models apply e.g. stochastic programming (SO) that assumes perfect knowledge on parameter distribution. For example, [41] presented an energy scheduling strategy of the MG operation based on the probabilistic forecasts of both the wind power and the user's demand. [42] proposed a stochastic optimization framework for smart home energy management while considering the uncertainty associated with the RES generation and the plug-in electric vehicle's plug-state. The stochastic based approaches often require high computational effort due to the significant number of scenarios, which limits their performance.

Robust optimization (RO) has been extensively used, as an alternative to SO as it has significantly better computational performance and simpler uncertainty modelling [18]. RO method that considers the worst-case scenario is utilized frequently in this context [43, 44, 45, 46]. In contrast to AIROBE, this work is conservative as it protects against the uncertainty risk assuming that all uncertain parameters may deviate to their worst value at the same time, which may be very unlikely in practice. The authors in [47] investigated the energy management in MGs in relation with the uncertainty derived

from the energy price signals, which differs from our work that focuses on the uncertainty on the PV generation and the load side, given a budget of uncertainty. A robust optimization approach with adjustable robustness level is adopted in [48], which does not consider uncertainties in RES generation and price volatility.

In recent work of [49], the authors presented a quadratic min-max robust solution under the cardinality-constrained uncertainty set based on the classical Gamma robustness theory [18] for energy management of a residential MG under uncertainties on demand and renewable power generation. The proposed solution protects against the worst-case scenario, based on symmetric deviation ranges with fixed uncertainty. Similarly, in [50] the authors propose robust energy scheduling solution for a smart building under PV generation uncertainty. The authors also use the budget of uncertainty based model and consider PV output forecasting as an input, and they assume that the upper and lower bounds deviate 20% from the forecasted values. In contrast, our work introduces favourable deviations and incorporates time-varying and asymmetrical uncertainty ranges.

8. Conclusion

In this paper we presented AIROBE, a MGs energy management robust optimization model that schedules the MGs operations under PV power generation and consumption uncertainties, in an effective and opportunistic manner. We use time-series prediction technique using clustering in order to forecast PV power generation and energy demand that are needed for the model input. We discussed the limitations of the classical worst-case robust optimization based approach and motivated the need to integrate more accurate uncertainty ranges, i,e, asymmetric and time-varying deviation ranges. We proposed a less conservative robust approach that accounts for the good deviations in a MG and demonstrated that AIROBE reduces the Price of Robustness while maintaining the same level of protection.

Acknowledgements

This work has been partly funded by the Energy Agency of Sweden (Energimyndigheten) through the AI4-ENERGI project (Projektnr: 50246-1).

References

[1] F. Farzan, S. Lahiri, M. Kleinberg, K. Gharieh, M. Jafari, Microgrids for fun and profit: The economics of installation investments and operations, Power and Energy Magazine, IEEE 11 (2013) 52–58.

[2] T. S. Ustun, C. Ozansoy, A. Zayegh, Recent developments in microgrids and example cases around the world—a review, Renewable and Sustainable Energy Reviews 15 (8) (2011) 4030–4041.

[3] Z. Liu, Q. Wu, S. Huang, H. Zhao, Transactive energy: A review of state of the art and implementation, in: 2017 IEEE Manchester PowerTech, 2017, pp. 1–6.

[4] R. H. Lasseter, P. Paigi, Microgrid: a conceptual solution, 2004 IEEE 35th Annual Power Electronics Specialists Conference (IEEE Cat. No.04CH37551) 6 (2004) 4285–4290 Vol.6.

[5] N. Hatziargyriou, H. Asano, R. Iravani, C. Marnay, Microgrids, IEEE Power and Energy Magazine 5 (4) (2007) 78–94.

[6] J. M. Raya-Armenta, N. Bazmohammadi, J. G. Avina-Cervantes, D. Sáez, J. C. Vasquez, J. M. Guerrero, Energy management system optimization in islanded microgrids: An overview and future trends, Renewable and Sustainable Energy Reviews 149 (2021) 111327.

[7] C. C. S. D. T. C. L. G. Hu, Smart energy management system for optimal microgrid economic operation, Wiley and The Institution of Engineering and Technology 5 (3) (2011) 258 – 267.

[8] A. Agüera-Pérez, J. C. Palomares-Salas, J. J. González de la Rosa, O. Florencias-Oliveros, Weather forecasts for microgrid energy management: Review, discussion and recommendations, Applied Energy 228 (2018) 265–278.

[9] P. Samadi, H. Mohsenian-Rad, V. W. S. Wong, R. Schober, Tackling the load uncertainty challenges for energy consumption scheduling in smart grid, IEEE Transactions on Smart Grid 4 (2) (2013) 1007–1016.

[10] N. Liu, X. Yu, C. Wang, C. Li, L. Ma, J. Lei, Energy-sharing model with price-based demand response for microgrids of peer-to-peer prosumers, IEEE Transactions on Power Systems 32 (5) (2017) 3569–3583.

[11] J. Barton, D. Infield, Energy storage and its use with intermittent renewable energy, IEEE Transactions on Energy Conversion 19 (2) (2004) 441–448.

[12] R. Dufo-López, J. L. Bernal-Agustín, J. Contreras, Optimization of control strategies for stand-alone renewable energy systems with hydrogen storage, Renewable Energy 32 (7) (2007) 1102–1126.

[13] Z. Liao, A. Parisio, Reliability optimization of multi-energy system considering energy storage devices effects under weather uncertainties, Energies 15 (3) (2022).

[14] A. Molderink, V. Bakker, M. G. C. Bosman, J. L. Hurink, G. J. M. Smit, Management and control of domestic smart grid technology, IEEE Transactions on Smart Grid 1 (2) (2010) 109–119.

[15] A. Nammouchi, P. Aupke, A. Kassler, A. Theocharis, V. Raffa, M. D. Felice, Integration of AI, IoT and Edge-Computing for Smart Microgrid Energy Management, in: 2021 IEEE International Conference on Environment and Electrical Engineering and 2021 IEEE Industrial and Commercial Power Systems Europe (EEEIC / ICPS Europe), 2021, pp. 1–6.

[16] P. Aupke, A. Kassler, A. Theocharis, M. Nilsson, I. M. Andersson, Impact of clustering methods on machine learning-based solar power prediction models, in: 2022 IEEE International Smart Cities Conference (ISC2), 2022, pp. 1–7.

[17] C. Zhang, Y. Xu, Z. Y. Dong, K. P. Wong, Robust coordination of distributed generation and price-based demand response in microgrids, IEEE Transactions on Smart Grid 9 (5) (2018) 4236–4247.

[18] D. Bertsimas, M. Sim, The price of robustness, Operations Research 52 (1) (2004) 35–53.

[19] D. Bertsimas, D. B. Brown, C. Caramanis, Theory and applications of robust optimization, SIAM Review 53 (3) (2011) 464–501.

[20] C. Büsing, F. D'Andreagiovanni, New results about multi-band uncertainty in robust optimization, in: R. Klasing (Ed.), Experimental Algorithms, Springer, Berlin, Heidelberg, 2012, pp. 63–74.

[21] E. Isaksson, M. Karpe Conde, Solar power forecasting with machine learning techniques (2018).

[22] P. Aupke, A. Kassler, A. Theocharis, M. Nilsson, M. Uelschen, Quantifying uncertainty for predicting renewable energy time series data using machine learning (2021).

[23] C. A. Ratanamahatana, E. Keogh, Making time-series classification more accurate using learned constraints, in: Proceedings of the 2004 SIAM international conference on data mining, SIAM, 2004, pp. 11–22.

[24] G. Ke, Q. Meng, T. Finley, T. Wang, W. Chen, W. Ma, Q. Ye, T.-Y. Liu, Lightgbm: A highly efficient gradient boosting decision tree, Advances in neural information processing systems 30 (2017).

[25] E. Al Daoud, Comparison between xgboost, lightgbm and catboost using a home credit dataset, International Journal of Computer and Information Engineering 13 (1) (2019) 6–10.

[26] C. Chen, Q. Zhang, Q. Ma, B. Yu, Lightgbm-ppi: Predicting protein-protein interactions through lightgbm with multi-information fusion, Chemometrics and Intelligent Laboratory Systems 191 (2019) 54–64.

[27] Y. Cao, L. Gui, Multi-step wind power forecasting model using lstm networks, similar time series and lightgbm, in: 2018 5th International Conference on Systems and Informatics (ICSAI), IEEE, 2018, pp. 192–197.

[28] R. Koenker, K. F. Hallock, Quantile regression, Journal of economic perspectives 15 (4) (2001) 143–156.

[29] W. Zhang, H. Quan, D. Srinivasan, Parallel and reliable probabilistic load forecasting via quantile regression forest and quantile determination, Energy 160 (2018) 810–819.

[30] M. A. Jirdehi, V. S. Tabar, S. Ghassemzadeh, S. Tohidi, Different aspects of microgrid management: A comprehensive review, Journal of Energy Storage 30 (2020) 101457.

[31] M. F. Zia, E. Elbouchikhi, M. Benbouzid, Microgrids energy management systems: A critical review on methods, solutions, and prospects, Applied Energy 222 (2018) 1033–1055.

[32] Z. Wang, B. Chen, J. Wang, M. Begovic, C. Chen, Coordinated energy management of networked microgrids in distribution systems, IEEE Transactions on Smart Grid 6 (2015) 45–53.

[33] D. Papadaskalopoulos, D. Pudjianto, G. Strbac, Decentralized coordination of microgrids with flexible demand and energy storage, Sustainable Energy, IEEE Transactions on 5 (2014) 1406–1414.

[34] J. Shin, J. H. Lee, M. J. Realff, Operational planning and optimal sizing of microgrid considering multi-scale wind uncertainty, Applied Energy 195 (2017) 616–633.

[35] J. Pascual, J. Barricarte, P. Sanchis, L. Marroyo, Energy management strategy for a renewable-based residential microgrid with generation and demand forecasting, Applied Energy 158 (2015) 12–25.

[36] E. Mortaz, J. Valenzuela, Microgrid energy scheduling using storage from electric vehicles, Electric Power Systems Research 143 (2017) 554–562.

[37] C. Battistelli, Y. P. Agalgaonkar, B. C. Pal, Probabilistic dispatch of remote hybrid microgrids including battery storage and load management, IEEE Transactions on Smart Grid 8 (3) (2017) 1305 – 1317.

[38] P. M. F. S. F. L. Benjamin Heymann, J. Frederic Bonnans, Continuous optimal control approaches to microgrid energy management, Energy Systems, Springer 9 (2018) 59–77.

[39] A. Askarzadeh, A memory-based genetic algorithm for optimization of power generation in a microgrid, IEEE Transactions on Sustainable Energy 9 (3) (2018) 1081–1089.

[40] A. Takeuchi, T. Hayashi, Y. Nozaki, T. Shimakage, Optimal scheduling using metaheuristics for energy networks, IEEE Transactions on Smart Grid 3 (2) (2012) 968–974.

[41] P. Kou, D. Liang, L. Gao, Stochastic energy scheduling in microgrids considering the uncertainties in both supply and demand, IEEE Systems Journal 12 (3) (2018) 2589–2600.

[42] X. Wu, X. Hu, X. Yin, S. J. Moura, Stochastic optimal energy management of smart home with pev energy storage, IEEE Transactions on Smart Grid 9 (3) (2018) 2065–2075.

[43] L. Wang, Q. Li, R. Ding, M. Sun, G. Wang, Integrated scheduling of energy supply and demand in microgrids under uncertainty: A robust multi-objective optimization approach, Energy 130 (2017) 1–14.

[44] C. Zhang, Y. Xu, Z. Y. Dong, J. Ma, Robust operation of microgrids via two-stage coordinated energy storage and direct load control, IEEE Transactions on Power Systems 32 (4) (2017) 2858–2868.

[45] G. Liu, M. Starke, B. Xiao, X. Zhang, K. Tomsovic, Microgrid optimal scheduling with chance-constrained islanding capability, Electric Power Systems Research 145 (2017) 197–206.

[46] G. Liu, M. Starke, B. Xiao, K. Tomsovic, Robust optimization based microgrid scheduling with islanding constraints, IET Generation, Transmission Distribution 11 (02 2017).

[47] A. Hussain, V.-H. Bui, H.-M. Kim, Robust optimal operation of ac/dc hybrid microgrids under market price uncertainties, IEEE Access 6 (2018) 2654–2667.

[48] C. Wang, Y. Zhou, B. Jiao, Y. Wang, W. Liu, D. Wang, Robust optimization for load scheduling of a smart home with photovoltaic system, Energy Conversion and Management 102 (2015) 247–257.

[49] S. M. Hosseini, R. Carli, M. Dotoli, Robust optimal energy management of a residential microgrid under uncertainties on demand and renewable power generation, IEEE Transactions on Automation Science and Engineering 18 (2) (2021) 618–637. doi:10.1109/TASE.2020.2986269.

[50] Z. Foroozandeh, I. Tavares, J. Soares, S. Ramos, Z. Vale, Robust energy scheduling for smart buildings considering uncertainty in pv generation, in: 2022 9th International Conference on Electrical and Electronics Engineering (ICEEE), 2022, pp. 245–249. doi:10.1109/ICEEE55327.2022.9772561.

Appendix A. Proofs

We provide here the proof of Proposition 1.

Proposition. *For each time period $t \in T$, the robust counterpart of constraint* (9) *when protection for Γ_t^{PV} "bad" deviations and Θ_t^{PV} "good" deviations of PV generation coefficients and Γ_t^{PC} "bad" deviations and Θ_t^{PC} "good" deviations of load coefficients are allowed in period t writes as:*

$$\sum_{j\in C}\left[\bar{p}_{j,t}^{PV} + \left(b_{j,t}^{dis} - b_{j,t}^{ch}\right)\right] - \left(\Gamma_t^{PV}\cdot v_t^{PV-} - \Theta_t^{PV}\cdot v_t^{PV+} + \sum_{j\in C} w_{j,t}^{PV}\right)$$
$$+\left(p_t^{imp} - p_t^{exp}\right) \geq \sum_{j\in C}\bar{p}_{j,t}^{PC} + \left(\Gamma_t^{PC}\cdot v_t^{PC+} - \Theta_t^{PC}\cdot v_t^{PC-} + \sum_{j\in C} w_{j,t}^{PC}\right) \tag{A.1}$$

$$v_t^{PV-} + w_{j,t}^{PV} \geq \delta_{j,t}^{PV-} \qquad \forall j \in C \tag{A.2}$$
$$-v_t^{PV+} + w_{j,t}^{PV} \geq -\delta_{j,t}^{PV+} \qquad \forall j \in C \tag{A.3}$$
$$v_t^{PC+} + w_{j,t}^{PC} \geq \delta_{j,t}^{PC+} \qquad \forall j \in C \tag{A.4}$$
$$-v_t^{PC-} + w_{j,t}^{PC} \geq -\delta_{j,t}^{PC-} \qquad \forall j \in C \tag{A.5}$$
$$v_t^{PV+},\ v_t^{PV-} \geq 0 \tag{A.6}$$
$$w_{j,t}^{PV} \geq 0 \qquad \forall j \in C \tag{A.7}$$
$$v_t^{PC+},\ v_t^{PC-} \geq 0 \tag{A.8}$$
$$w_{j,t}^{PC} \geq 0 \qquad \forall j \in C \tag{A.9}$$

Proof. In order to prove this result, we first focus attention on a time period $t \in T$ and define a robust version of the constraint load satisfaction constraint (9) in which we include terms:

- $-DEV(\Gamma_t^{PV}, \Theta_t^{PV})$ to represent the worst decrease that the left-hand-side of the constraint may experience for Γ_t^{PV} bad deviations and Θ_t^{PV} good deviations of the PV coefficients;
- $+DEV(\Gamma_t^{PC}, \Theta_t^{PC})$ to represent the worst increase that the right-hand-side of the constraint may experience for Γ_t^{PC} bad deviations and Θ_t^{PC} good deviations of the load coefficients.

This constraint writes as:

$$\sum_{j\in C}\left[\bar{p}_{j,t}^{PV} + \left(b_{j,t}^{dis} - b_{j,t}^{ch}\right)\right] - DEV(\Gamma_t^{PV}, \Theta_t^{PV}) + \left(p_t^{imp} - p_t^{exp}\right) \geq \sum_{j\in C}\bar{p}_{j,t}^{PC} \tag{A.10}$$

The value $DEV(\Gamma_t^{PV}, \Theta_t^{PV})$ corresponds to the optimal value of the following combinatorial optimization problem:

$$DEV(\Theta_t^{PV}, \Gamma_t^{PV}) = \max \sum_{j\in C}\left(\delta_{j,t}^{PV-}\cdot z_{j,t}^{-} - \delta_{j,t}^{PV+}\cdot z_{j,t}^{+}\right) \tag{A.11}$$
$$\sum_{j\in C} z_{j,t}^{PV-} \leq \Gamma_t^{PV} \tag{A.12}$$
$$\sum_{j\in C} z_{j,t}^{PV+} \geq \Theta_t^{PV} \tag{A.13}$$
$$z_{j,t}^{PV-} + z_{j,t}^{PV+} \leq 1 \qquad \forall j \in C \tag{A.14}$$
$$z_{j,t}^{PV-} \in \{0,1\} \qquad \forall j \in C \tag{A.15}$$
$$z_{j,t}^{PV+} \in \{0,1\} \qquad \forall j \in C \tag{A.16}$$

in which:

- a binary variable $z_{j,t}^{PV-}$ (A.15) is equal to 1 if coefficient $\bar{p}_{j,t}^{PV}$ experiences the largest bad deviation (decrease of PV generation) $\delta_{j,t}^{PV-}$ and to 0 otherwise;
- a binary variable $z_{j,t}^{PV+}$ (A.16) is equal to 1 if coefficient $\bar{p}_{j,t}^{PV}$ experiences the largest good deviation (increase of PV generation) $\delta_{j,t}^{PV+}$ and to 0 otherwise;
- the constraint (A.12) imposes that at most Γ_t^{PV} bad deviations may occur;
- the constraint (A.13) imposes that at least Θ_t^{PV} good deviations must occur;
- the constraints (A.14) impose that each coefficient may experience at most one kind of deviation (either bad or good);
- the objective function (A.11) pursues the maximization of the worst reduction in value of the left-hand-side of constraint due to the summation of bad and good deviations;

Let us now consider the linear relaxation of the previous combinatorial optimization problem, i.e. the following problem in which the integrality requirement (A.15), (A.16) on the binary variables is removed and they can assume any value between 0 and 1:

$$DEV(\Theta_t^{PV}, \Gamma_t^{PV}) = \max \sum_{j \in C} \left(\delta_{j,t}^{PV-} \cdot z_{j,t}^{-} - \delta_{j,t}^{PV+} \cdot z_{j,t}^{+} \right) \tag{A.17}$$

$$\sum_{j \in C} z_{j,t}^{PV-} \leq \Gamma_t^{PV} \tag{A.18}$$

$$\sum_{j \in C} z_{j,t}^{PV+} \geq \Theta_t^{PV} \tag{A.19}$$

$$z_{j,t}^{PV-} + z_{j,t}^{PV+} \leq 1 \qquad \forall j \in C \tag{A.20}$$

$$0 \leq z_{j,t}^{PV-} \leq 1 \qquad \forall j \in C \tag{A.21}$$

$$0 \leq z_{j,t}^{PV+} \leq 1 \qquad \forall j \in C \tag{A.22}$$

It can be noted that its bínary coefficient matrix is totally unimodular [20]. Consequently, the optimal solution of the linear relaxation problem is integral and provides an optimal solution also for the combinatorial optimization problem.
We can then define the dual problem of the linear relaxation:

$$DEV(\Theta_t^{PV}, \Gamma_t^{PV}) = \min \ \Gamma_t^{PV} \cdot v_t^{PV-} - \Theta_t^{PV} \cdot v_t^{PV+} + \sum_{j \in C} w_{j,t}^{PV} \tag{A.23}$$

$$v_t^{PV-} + w_{j,t}^{PV} \geq \delta_{j,t}^{PV-} \qquad \forall j \in C \tag{A.24}$$

$$-v_t^{PV+} + w_{j,t}^{PV} \geq -\delta_{j,t}^{PV+} \qquad \forall j \in C \tag{A.25}$$

$$v_t^{PV+}, \ v_t^{PV-} \geq 0 \tag{A.26}$$

$$w_{j,t}^{PV} \geq 0 \qquad \forall j \in C \tag{A.27}$$

$$\tag{A.28}$$

By duality theory, since the linear relaxation (A.17)-(A.22) is finite and optimal, also its dual problem (A.23)-(A.27) is finite and optimal and the optimal values of the two problems coincide. Consequently, we can use the dual problem to substitute the term $DEV(\Gamma_t^{PV}, \Theta_t^{PV})$ in the robust constraint (Appendix A), as specified in [20].

We can proceed in the same way for dealing with the deviation term $+DEV(\Gamma_t^{PC}, \Theta_t^{PC})$ appearing in the right-hand-side of the constraint (9). Specifically, the value $DEV(\Gamma_t^{PC}, \Theta_t^{PC})$ corresponds to the optimal value of the following combinatorial optimization problem:

$$DEV(\Theta_t^{PC}, \Gamma_t^{PC}) = \max \sum_{j \in C} \left(\delta_{j,t}^{PC+} \cdot z_{j,t}^{+} - \delta_{j,t}^{PC-} \cdot z_{j,t}^{-} \right) \tag{A.29}$$

$$\sum_{j \in C} z_{j,t}^{PC+} \leq \Gamma_t^{PC} \tag{A.30}$$

$$\sum_{j \in C} z_{j,t}^{PC-} \geq \Theta_t^{PC} \tag{A.31}$$

$$z_{j,t}^{PC-} + z_{j,t}^{PC+} \leq 1 \qquad \forall j \in C \tag{A.32}$$

$$z_{j,t}^{PC-} \in \{0, 1\} \qquad \forall j \in C \tag{A.33}$$

$$z_{j,t}^{PC+} \in \{0, 1\} \qquad \forall j \in C \tag{A.34}$$

in which:

- a binary variable $z_{j,t}^{PC-}$ (A.33) is equal to 1 if coefficient $\bar{p}_{j,t}^{PC}$ experiences the largest good deviation (decrease of load) $\delta_{j,t}^{PC-}$ and to 0 otherwise;
- a binary variable $z_{j,t}^{PC+}$ (A.34) is equal to 1 if coefficient $\bar{p}_{j,t}^{PC}$ experiences the largest bad deviation (increase of load) $\delta_{j,t}^{PV+}$ and to 0 otherwise;
- the constraint (A.30) imposes that at most Γ_t^{PC} bad deviations may occur;
- the constraint (A.31) imposes that at least Θ_t^{PC} good deviations must occur;
- the constraints (A.32) impose that each coefficient may experience at most one kind of deviation (either bad or good);
- the objective function (A.29) pursues the maximization of the worst increase in value of the right-hand-side of constraint due to the summation of bad and good deviations;

Also for the previous combinatorial optimization problem, we can define its linear relaxation, removing the integrality requirement on the binary variables:

$$DEV(\Theta_t^{PC}, \Gamma_t^{PC}) = \max \sum_{j \in C} \left(\delta_{j,t}^{PV+} \cdot z_{j,t}^{+} - \delta_{j,t}^{PV-} \cdot z_{j,t}^{-} \right) \tag{A.35}$$

$$\sum_{j \in C} z_{j,t}^{PV+} \leq \Gamma_t^{PC} \tag{A.36}$$

$$\sum_{j \in C} z_{j,t}^{PC-} \geq \Theta_t^{PC} \tag{A.37}$$

$$z_{j,t}^{PC-} + z_{j,t}^{PC+} \leq 1 \qquad \forall j \in C \tag{A.38}$$

$$0 \leq z_{j,t}^{PC-} \leq 1 \qquad \forall j \in C \tag{A.39}$$

$$0 \leq z_{j,t}^{PC+} \leq 1 \qquad \forall j \in C \tag{A.40}$$

In this case, the bínary coefficient matrix is also totally unimodular [20] and thus the optimal solution of the linear relaxation problem is integral and provides an optimal solution also for the

combinatorial optimization problem.
Therefore, we can define the dual problem of the linear relaxation:

$$DEV(\Theta_t^{PC}, \Gamma_t^{PC}) = \min \ \Gamma_t^{PC} \cdot v_t^{PC+} - \Theta_t^{PC} \cdot v_t^{PC-} + \sum_{j \in C} w_{j,t}^{PC} \tag{A.41}$$

$$v_t^{PC+} + w_{j,t}^{PC} \geq \delta_{j,t}^{PC+} \qquad \forall j \in C \tag{A.42}$$

$$-v_t^{PC-} + w_{j,t}^{PC} \geq -\delta_{j,t}^{PC-} \qquad \forall j \in C \tag{A.43}$$

$$v_t^{PC+}, \ v_t^{PC-} \geq 0 \tag{A.44}$$

$$w_{j,t}^{PC} \geq 0 \qquad \forall j \in C \tag{A.45}$$

$$\tag{A.46}$$

Finally, we can use the dual problems (A.23)-(A.27) and (A.41)-(A.45) to substitute the terms $DEV(\Gamma_t^{PV}, \Theta_t^{PV})$ and $DEV(\Gamma_t^{PC}, \Theta_t^{PC})$ in, thus obtaining the robust optimization model (A.1)-(A.9) and completing the proof. □